

# Design Considerations and Prototype Performance of the Fermilab Main Injector Dipole

D. J. Harding, M. E. Bleadon, B. C. Brown, E. Desavouret, J. D. Garvey, H. D. Glass, F. A. Harfoush, S. D. Holmes, J. C. Humbert, J. M. Jagger, G. R. Kobliska, A. Lipski, P. S. Martin, P. O. Mazur, F. E. Mills, D. F. Orris, J.-F. Ostiguy, S. G. Peggs, J. E. Pachnik, E. E. Schmidt, J. W. Sim, S. C. Snowdon, and D. G. Walbridge  
*Fermi National Accelerator Laboratory\**

*P.O. Box 500*

*Batavia, Illinois 60510*

## Abstract

The Main Injector project at Fermilab requires a dipole with good field quality from 0.1 T to 1.73 T with ramps to full field at up to 2.4 T/s over an aperture of 10x5 cm. Operation of this magnet for the variety of purposes proposed for the Main Injector results in a design with low inductance, large copper cross section, and field uniformity sufficient for high intensity injection and efficient slow resonant extraction. The resulting design is presented, along with measurement results of a prototype magnet emphasizing the field uniformity.

## 1 Introduction

The Fermilab Main Injector is designed to replace the Fermilab Main Ring with a ring of new and recycled magnets in a new tunnel[1][2]. The largest new component will be the dipole magnets. These magnets are tailored to the needs of the project. They are conventional magnets, with a core of iron laminations and a conductor of water-cooled copper. The machine can run as rapidly as 1.5 seconds/cycle during anti-proton production. The basic magnet parameters are presented in Table 1. We have built and measured one prototype magnet.

## 2 Design Requirements

The ring is required to transmit a beam with  $40\pi$  mm-mr normalised emittance and a momentum spread of  $\pm 1.4\%$  at transition. The dipole field ranges from 0.1 Tesla at injection to 1.72 T at 150 GeV. The lengths are 6 and 4 meters. Three factors have led us to decide to build new dipoles, rather than reusing the Main Ring dipoles: geometric aperture, dynamic aperture, and operational reliability.

|                 | "6-meter"                           | "4-meter"      |
|-----------------|-------------------------------------|----------------|
| Length          | 240 inches                          | 160 inches     |
| Sagitta         | 16 mm                               | 7 mm           |
| Number          | 216                                 | 128            |
| Color           | light blue                          |                |
| Gap             | 5.08 cm (2 inch)                    |                |
| Maximum field   | 1.73 T                              |                |
| Weight          | 17000 kg                            | 12000 kg       |
| Laminations     | 8000                                | 5333           |
| Conductor       | 2.54 x 10.16 cm <sup>2</sup> copper |                |
| Cooling water   | 1.27 cm dia. hole, 10.8 gpm         |                |
| Maximum current | 9420 A                              |                |
| Resistance      | 0.8 m $\Omega$                      | 0.6 m $\Omega$ |
| Inductance      | 2.0 mH                              | 1.3 mH         |
| Maximum ramp    | 240 GeV/sec (15000 A/sec)           |                |
| Peak power      | 75 kW                               | 50 kW          |

Table 1: Main Injector Dipole Parameters

We require the Main Injector to transport an increased emittance and momentum spread over what is possible in the Main Ring. Several aspects of lattice design have contributed to relaxing what would have been very difficult problems if we were just copying the Main Ring lattice. The increased density of quadrupoles has reduced the beta functions around the ring and thus the beam size for a given emittance. The reduced horizontal dispersion has reduced the horizontal aperture requirements for a given momentum spread.

The geometrical aperture is improved by building curved magnets to replace the straight Main Ring dipoles. The bending radius of the beam in the dipoles is about 290 meters. This produces an offset of 16 mm from the center line in the middle of a 6-meter dipole and an offset of 7 mm in the 4-meter dipoles. The magnet laminations, the good field region, and the beam pipe will follow that bend.

Dynamic aperture effects in the Main Ring dominate the losses at injection, where the beam is largest and losses are highest. Today's design tools have allowed us to design a magnet with much better field uniformity at the injection energy than is available in the Main Ring dipoles.

\*Operated by the Universities Research Association under contract with the U. S. Department of Energy

Experience has also allowed us to design a more reliable magnet. Most of the failures in the Main Ring dipoles occur at conductor joints within the coil. We have reduced the number of joints and improved the techniques used to braze the joints. The stresses on the coil joints are also reduced by allowing the coil to expand longitudinally in response to thermal cycles, rather than potting it in the core.

Within the requirements, we have minimized the sum of the construction cost and the operating cost over five years. The resulting cross section is shown in Figure 1. The gap is the same as the current Main Ring B2 dipole, but the copper area has been doubled. The number of turns has been reduced to eight, doubling the current required but reducing the inductance (to help achieve the increased ramp rate).

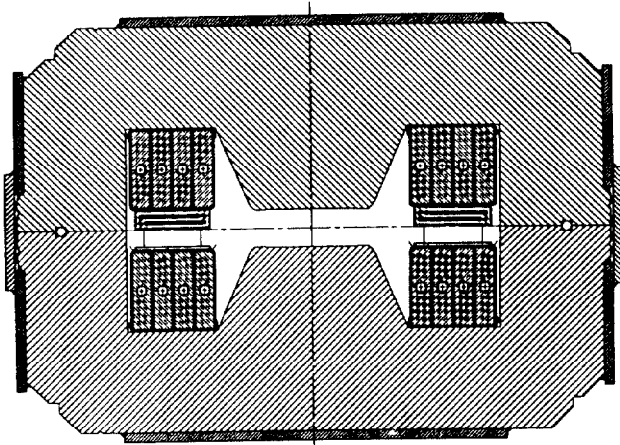


Figure 1: Cross section of Main Injector Dipole

### 3 Magnetic Field Requirements

The good field requirements vary through the accelerator cycle. At injection the beam is at its largest vertically and is also large horizontally. At transition (19 GeV) the increased momentum spread interacts with the dispersion (2 m) to let the beam continue to explore a large fraction of the horizontal aperture. The Main Injector sits at 120 GeV briefly during fast extraction for antiproton production and for 1.0 second during slow extraction to the fixed target area. The Main Injector ramps to 150 GeV (1.72 T) to accelerate protons and antiprotons for injection into the Tevatron. In collider mode the flattop is 2.4 seconds to allow for coalescing and cogging of beam bunches.

We ask that the field deviate no more than one part in  $10^4$  over a region that depends on the beam size. The required good field apertures are shown in Table 2. We ask also that the deviations from a uniform field be dominated

| Energy  | Field  | Horizontal  | Vertical    |
|---------|--------|-------------|-------------|
| 8 GeV   | 0.1 T  | $\pm 21$ mm | $\pm 23$ mm |
| 19 GeV  | 0.22 T | $\pm 21$ mm | $\pm 21$ mm |
| 120 GeV | 1.38 T | $\pm 30$ mm | $\pm 10$ mm |
| 150 GeV | 1.72 T | $\pm 11$ mm | $\pm 9$ mm  |

Table 2: Required good field region as a function of energy

by the sextupole field component to permit compensation of the errors by the sextupoles alone, avoiding higher order correction elements.

We include a small positive sextupole component in the lamination shape to partially compensate for the saturation at higher fields. (The net sextupole is 0 at approximately 0.83 T.) The remnant field (12 gauss) is sufficiently small compared to the injection field that the modest variations in the remnant field do not seriously disrupt the field shape.

The design goal for the magnet end is to provide a "neutral" end field. Measurements of the prototype magnet confirm the computations discussed in Reference [6].

A ramping dipole magnet induces eddy currents in its conductive beam pipe, which in turn produce a sextupole magnetic field. We have calculated[3] the fields for the expected operation of the Main Injector and find them to be a significant effect, but not so severe as to require active compensation within the magnet.

### 4 Magnetic Field Measurements

We have measured the magnetic field using the Fermilab Magnet Test Facility's repertoire of measurement systems[4]. This includes NMR probes, Hall probes, rotating coils, and "flatcoil" (a long narrow coil which is only translated, not rotated).

We have measured the field of the prototype magnet as a function of current using standard Hall probe, NMR, and rotating coil techniques. The transfer function, B/I is plotted in Figure 2. The NMR probe sample is sensitive over the range 1.25 T to 1.80 T. The Hall probe has been calibrated to match the NMR over this range and extend the measurement to lower fields. The absolute calibration of the rotating coil measurement depends on the geometrical constants of the probe, especially the probe radius. These are only measured reliably to about the 0.3% precision suggested by the agreement between the strength measurements.

We have measured the body field of the first prototype magnet to validate the lamination design. The measured magnetic field is plotted in Figure 3 for injection, 120 GeV, and 150 GeV.

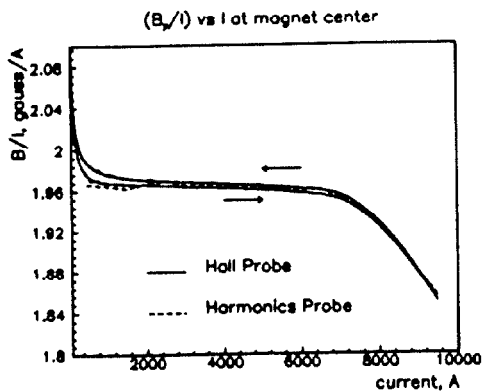


Figure 2: Magnetic field/Current for Main Injector Dipole

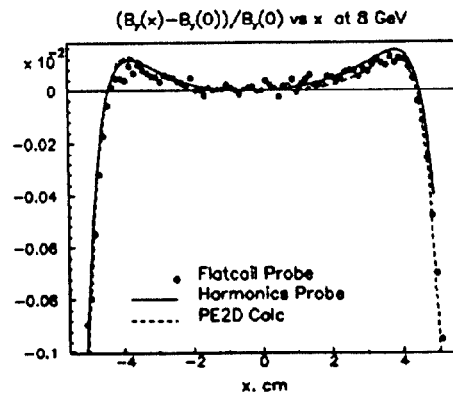


Figure 4:  $B_Y(x)$  at  $y=0$  cm and  $B(0)=0.10$  T computed, measured with flatcoil, and recreated from harmonics

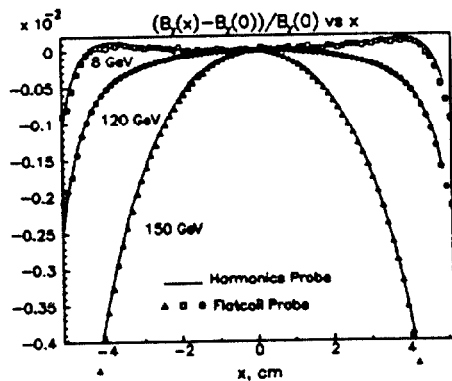


Figure 3:  $B_Y(x)$  for Main Injector Dipole at Injection, 120 GeV, and 150 GeV

Figure 4 shows the field  $B_Y(x)$  at  $y=0$  and  $B(0)=0.10$  T. Shown are the field as calculated [5], as measured with the flatcoil system, and as reconstituted from three rotating coil harmonic measurements. The agreement is strikingly good, both here and off the midplane. Excellent agreement continues through the range of field strengths where the steel remains, at most, only mildly saturated.

At high fields we find the agreement among the measurements techniques (flatcoil, harmonics, Hall, and NMR) to remain excellent. The agreement with calculation is not as good, with the calculated deviation of the field from its central value typically 25% less than the measured deviation. We attribute the differences to our lack of knowledge of the B-H curve of the steel above 100 Oersted (about 1.8 T). The bumps toward the edges of the pole face, which help contain the field lines and contribute to uniformity at low field, saturate first as the field rises. At full excitation the field in the bumps is well over 2 T. Since the field shape is dominated by those bumps, small errors in the extrapolation of the B-H curve have a large effect in the predicted field shape.

## 5 Acknowledgements

Many groups at Fermilab have contributed to this work. We would especially like to thank Arnie Knauf of Technical Support Engineering; Ray Carra and Don Olson for design efforts; and Shree Agrawal, Steve Helis, Keith Dillow, Cervando Castro, Butch Bianchi, Dave Hartness, Mike Cherry, Mark Thompson, and Dean Validis from the Magnet Test Facility for fabrication and testing efforts.

## References

- [1] S. D. Holmes. Achieving high luminosity in the Fermilab Tevatron. In *Proceedings of the IEEE 1991 Particle Accelerator Conference*.
- [2] Fermilab Upgrade: Main Injector. Conceptual Design Report, March 1991. Revision 2.3, Addendum.
- [3] Jean-François Ostiguy. Eddy current induced multipoles in the Main Injector. Technical report, Fermilab Main Injector Note, October 1990. MI0037.
- [4] Bruce C. Brown. Fundamentals of magnetic measurements with illustrations from Fermilab experience. In P. F. Dahl, editor, *Proceedings of the ICFA Workshop on Superconducting Magnets and Cryogenics*, page 297. Brookhaven National Lab, 1986.
- [5] Jean-François Ostiguy. Main Injector dipole magnet: 2D field computations. Technical report, Fermilab Main Injector Note, October 1990. MI0036.
- [6] J.-F. Ostiguy. Magnet end design: The Main Injector dipoles. In *Proceedings of the IEEE 1991 Particle Accelerator Conference*.